Catalysis Today 153 (2010) 189–192

Contents lists available at ScienceDirect

Catalysis Today

journal homepage: www.elsevier.com/locate/cattod

Preparation of highly active platinum nanoparticles on ZSM-5 zeolite including cerium and titanium dioxides as photo-assisted deposition sites

Sayoko Shironita, Masahiko Goto, Takashi Kamegawa, Kohsuke Mori, Hiromi Yamashita*

Division of Materials and Manufacturing Science, Graduate School of Engineering, Osaka University, 2-1, Yamada-oka, Suita, Osaka 565-0871, Japan

ARTICLE INFO

Article history:
Available online 23 May 2010

Keywords:
Pt nanoparticle
CeO_2
UV-light irradiation
Photo-deposition

ABSTRACT

Nano-sized Pt particles with high activities for CO oxidation have been successfully synthesized on the metal dioxide phases (CeO_2 and TiO_2) included within ZSM-5 zeolite by a photo-assisted deposition (PAD) method under UV-light irradiation. The obtained Pt nanoparticles on CeO_2 within ZSM-5 by the PAD method (PAD-Pt/CeO_2/ZSM-5) showed the highest catalytic activity for CO oxidation even at low temperature. The dispersion of Pt nanoparticles was investigated by CO adsorption, XAFS, and TEM analyses. The size of Pt nanoparticle of the PAD-Pt/CeO_2/ZSM-5 catalyst was determined to be 2 nm. In addition, this catalyst has unique morphology; the Pt nanoparticles were selectively deposited on the CeO_2 within ZSM-5 supports. It is found that the addition of CeO_2 into the catalyst supports is effective to synthesize highly active nano-sized Pt particles using the PAD method under UV-light irradiation.

© 2010 Elsevier B.V. All rights reserved.

1. Introduction

Rhodium, platinum, palladium, ruthenium, and gold are one of the most expensive and noble metals in the industrial field, and values and costs of these metals are gradually increasing. However, these metals play a very important role as catalysts for many reactions, such as hydrogenation, dehydrogenation, oxidation, naphtha reforming, alcohol steam reforming, isomerization, hydrocracking, automobile exhaust removing and fuel cells [1–4]. In order to minimize the quantity of consumed precious metals, the development of novel method to prepare nano-sized and uniform metal particles with high activity is strongly desired.

Until now, metal particles have been supported on various metal oxides, such as silica, alumina, titania, and magnesia, to maintain particle size of metals and promote catalytic activities [4–7]. Porous materials exemplified by mesoporous silicas and zeolites have also been used as catalytic supports. These materials have high surface areas and are inactive under UV-light irradiation conditions, which provide reaction fields for photocatalytic and photochemical processes as reaction vessels [8].

Our previous works have proposed a photo-assisted deposition (PAD) method which is the novel technique to synthesize nano-sized metal particles (Pt, Pd, and PdAu) on Ti-containing mesoporous silica and Ti-containing zeolite under UV-light irradiation [9,10]. The excited state of Ti-oxide moieties within the silica frameworks under UV-light irradiation act as deposition sites of metal precursors such as Pt, Pd, and PdAu. The obtained catalysts by the PAD method exhibited high catalytic activities for NO decomposition and direct synthesis of hydrogen peroxide from H_2 and O_2.

In this work, metal oxide phases (CeO_2 and TiO_2) within ZSM-5 zeolite support were employed to prepare highly dispersed Pt nanoparticle under UV-light irradiation (Scheme 1). CeO_2 is used as co-catalyst in the automobile three-way catalyst because of its high oxygen storage capacity and stabilizing ability of precious metals. Moreover, CeO_2 and TiO_2 absorb visible and ultraviolet light as photocatalysts. It can be expected and herein demonstrated that CeO_2 and TiO_2 phases act as photo-assisted deposition sites to prepare nano-sized Pt nanoparticles under UV-light irradiation.

2. Experimental

2.1. Materials

ZSM-5 (molar ratio of $SiO_2/Al_2O_3 = 1900$) was kindly supplied from Tosoh Co. Ltd. Cerium (III) nitrate hexahydrate ($Ce(NO_3)_3{\cdot}6H_2O$, 98.0%), titanium tetraisopropoxide (TPOT: $Ti[OCH(CH_3)_2]_4$, 95.0%), 2-propanol ($(CH_3)_2CHOH$, 99.5%), hydrogen hexachloro platinate (IV) hexahydrate ($H_2PtCl_6{\cdot}6H_2O$, 98.5%) were purchased from Wako Pure Chemical Ind. Ltd. CeO_2 (JRC-CEO1) and TiO_2 (JRC-TIO6) were supplied from Catalysis Society of Japan. These materials were used without further purification.

* Corresponding author. Tel.: +81 6 6879 7457; fax: +81 6 6879 7457.
E-mail address: yamashita@mat.eng.osaka-u.ac.jp (H. Yamashita).

0920-5861/$ – see front matter © 2010 Elsevier B.V. All rights reserved.
doi:10.1016/j.cattod.2010.04.026

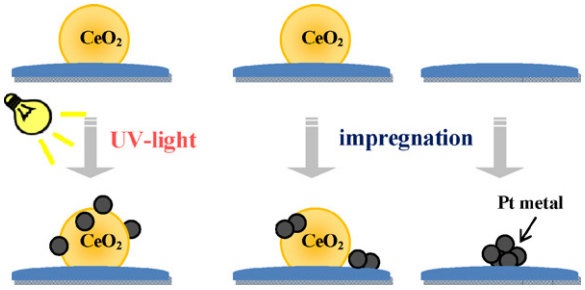

Scheme 1. Synthesis of Pt nanoparticles using a photo-assisted deposition method on CeO_2/ZSM-5 under UV-light irradiation and a conventional impregnation method.

2.2. Preparation of catalyst

ZSM-5 (3.0 g) was mixed with a 300 mL $Ce(NO_3)_3{\cdot}6H_2O$ aqueous solution (0.04 M) and stirred at room temperature for 0.5 h. The suspension was evaporated in vacuo, dried at 383 K for 18 h, and then calcined at 773 K for 5 h in air (CeO_2/ZSM-5, CeO_2: 5 wt%). Pt nanoparticles were deposited by two methods. CeO_2/ZSM-5 (0.4 g) was mixed with a 17.2 mL aqueous $H_2PtCl_6{\cdot}6H_2O$ solution (1.2 mM) in a quartz vessel at room temperature for 6 h with vigorous stirring under UV-light irradiation using a 100 W high pressure Hg lamp (wavelength: 253.7, 264.0, 300.2, 313.2, 365.0, 404.7, 435.8, 546.1, and 577.0 nm) by the photo-assisted deposition (PAD) method. After the filtration, the solid was dried at room temperature for 15 h under vacuum and calcined at 723 K for 5 h in air, giving a PAD-Pt/CeO_2/ZSM-5 (Pt: 0.5 wt%). In comparison, an imp-Pt/CeO_2/ZSM-5 catalyst was prepared by the conventional impregnation method (Pt: 0.5 wt%). A 50 mL of 2-propanol solution of titanium tetraisopropoxide ($Ti[OCH(CH_3)_2]_4$: 0.08 M) was used to deposit TiO_2 (5 wt%) on ZSM-5 instead of CeO_2, giving a PAD-Pt/TiO_2/ZSM-5 and an imp-Pt/TiO_2/ZSM-5.

2.3. Characterization

The powder X-ray diffraction (XRD) measurement was carried out by a RINT 2000 (Rigaku-denki) X-ray diffractometer using the Cu Kα radiation in step mode operated with 40 kV and 200 mA at 295 K. The Brunauer–Emmett–Teller (BET) surface area measurements were performed using N_2 adsorption–desorption by a BEL-SORP max (Bel Japan, Inc.) at 77 K. The sample was degassed under vacuum at 473 K for 3 h prior to data collection. The pore size distribution was calculated from N_2 desorption using the Molecular-Probe (MP) method. The inductively coupled plasma (ICP) measurement was performed using a Nippon Jarrell-Ash ICAP-575 Mark II instrument. Pt surface area and dispersion were evaluated by CO pulse chemisorption (CO/Pt = 1) by BEL-METAL-1 (Bel Japan, Inc.). The sample was pretreated under O_2 flow at 673 K for 15 min, and subsequently H_2 flow at 673 K for 15 min. The adsorption was measured at 323 K and CO flow rate was 20 mL min^{-1}. The UV–vis diffuse reflectance absorption spectrum was recorded with a UV-2450 (Shimadzu) UV–vis spectrophotometer at 295 K. TEM micrographs were obtained with a Hitachi H-800 TEM equipped with an energy-dispersive X-ray (EDX) detector, operated at 200 kV. Pt L_{III}-edge, Ce L_{III}-edge, and Ti K-edge X-ray absorption fine structure (XAFS) spectra were recorded using a fluorescence-yield collection technique at the beam line BL-7C station with an attached Si (1 1 1) monochromator of the Photon Factory at the High Energy Accelerator Research Organization, KEK, Tsukuba, Japan. The EXAFS data were normalized by fitting the background absorption coefficient, around the energy region higher than the edge of about 35–50 eV, with the smoothed absorption of an isolated atom. The EXAFS data were examined using the Rigaku EXAFS analysis program. Fourier transformation (FT) of k^3-weighted normalized EXAFS data was performed over the 3 Å < k ($Å^{-1}$) < 11 Å range to obtain the radial structure function.

Table 1
Results of N_2 adsorption–desorption measurement of support materials.

Sample	BET surface area ($m^2\ g^{-1}$)	Pore volume ($cm^3\ g^{-1}$)
ZSM-5	307	0.18
TiO_2/ZSM-5	299	0.19
CeO_2/ZSM-5	286	0.18

2.4. Catalytic reaction

CO oxidation was carried out using a fixed-bed reactor enclosed in a quartz-tube placed in an electronic furnace. The catalyst (100 mg) was placed in a quartz-tube reactor and pretreated under O_2 flow at 673 K for 15 min, and subsequently H_2 flow at 673 K for 15 min. The catalysis was carried out at desired temperature in a gaseous mixture of CO (0.33%), O_2 (0.16%), and He (balance) (total flow rate: 30 mL min^{-1}, SV = 18,000 mL $g_{cat}^{-1}\ h^{-1}$). The CO conversion was continuously monitored by a gas chromatograph GC-14B (Shimadzu) with thermal conductivity detector (TCD) equipped with Molecular Sieve 5A colums.

3. Results and discussion

There was no significant change for BET specific surface area and pore volume after deposition of CeO_2 and TiO_2 phases (Table 1), suggesting that the pore structure of ZSM-5 was retained and deposited CeO_2 and TiO_2 phases were existed in small particle size. Diffuse reflectance UV–vis spectra of the CeO_2/ZSM-5 and the TiO_2/ZSM-5 samples showed a shift of absorption edge toward shorter wavelength region than those of the corresponding bulk materials (Fig. 1), probably due to the quantum size effect [11]. In contrast, the Ce L_{III}-edge XANES spectrum of CeO_2/ZSM-5 resembled that of Ce^{4+} ion but differed from Ce^{3+} ion, suggesting that CeO_2 phase was formed [11]. The Ti K-edge XANES spectrum of TiO_2/ZSM-5 exhibited several pre-edge peaks at around 4970 eV. This result revealed that the Ti species exist not in isolated tetrahedrally coordination state but octahedral TiO_2 crystal structure [12]. In the XRD patterns, the peak due to CeO_2 (cubic) and TiO_2 (anatase) phases were observed, respectively [13,14]. The average crystal size of CeO_2 and TiO_2 were calaculated to be 20 nm by applying Scherrer's equation. This observation is well consistent with the results from TEM image as described below. From these results, it can be considered that these oxide phases were deposited on external surface of ZSM-5, which account for no change of BET surface area after deposition of metal dioxide phases. The absence of a metallic Pt phase in the XRD patterns suggested that the Pt particle sizes on CeO_2/ZSM-5 and TiO_2/ZSM-5 supports using the PAD method and

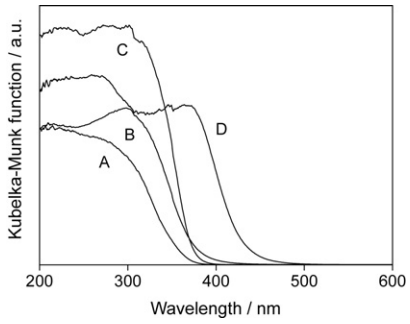

Fig. 1. UV–vis spectra of (A) TiO_2/ZSM-5, (B) CeO_2/ZSM-5, (C) TiO_2 bulk and (D) CeO_2 bulk.

Table 2
Pt metal dispersion and average particle size of Pt supported catalysts.

Sample	Metal dispersion (%)	Metal area ($m^2\ g^{-1}$)	Particle size (nm)
imp-Pt/ZSM-5	21	53	5.3
imp-Pt/TiO_2/ZSM-5	24	60	4.6
PAD-Pt/TiO_2/ZSM-5	34	84	3.3
imp-Pt/CeO_2/ZSM-5	39	97	2.9
PAD-Pt/CeO_2/ZSM-5	57	103	2.0

the impregnation method were too small to be detected by XRD due to the low Pt loadings. Table 2 shows the results of metal dispersion measurement using CO pulse chemisorption. The nano-sized small Pt particles were formed in all catalysts and PAD-Pt/CeO_2/ZSM-5 catalyst showed the smallest size among them. The size of Pt nanoparticles depended on the kind of supports and decreased in the order of ZSM-5 > TiO_2/ZSM-5 > CeO_2/ZSM-5. The PAD method produced smaller Pt nanoparticle compared to the impregnation one. Nagai et al. reported that interaction between Pt particle and metal oxide supports contributed to maintain Pt particle size and increased in the order of SiO_2 < Al_2O_3 < ZrO_2 < CeO_2 [15]. Their properties were demonstrated by the electron density of oxygen in the support oxide using observed by XPS measurement on the binding energy of the O(1s) electron. Therefore, the above results suggest that the Pt particle size on CeO_2/ZSM-5 was smaller due to the strong interaction between Pt nanoparticles and CeO_2 support. It is considered that the CeO_2 is effective support material for dispersion of Pt nanoparticles.

In an effort to compare the catalytic activities of the Pt metal nanoparticles deposited on CeO_2/ZSM-5 and TiO_2/ZSM-5, CO oxidation reaction were carried out at atmospheric pressure in the temperature range of 273–573 K, in a conventional fixed-bed reactor system. The results reported in Fig. 2 clearly suggest that the addition of CeO_2 and TiO_2 phases in the catalyst component significantly improved the catalytic performance. The temperature at 50% conversion decreased about 40 K by the addition of TiO_2 compared to impregnated Pt/ZSM-5 catalyst. In addition, the Pt deposited on TiO_2/ZSM-5 catalyst by the PAD method showed higher catalytic activity than that prepared by the impregnation one. The PAD method was found to be effective for the deposition of Pt nanoparticles on supports. The CeO_2 phase is more promotional catalytic activity for CO oxidation than the TiO_2 phase. Moreover, the Pt deposited on CeO_2/ZSM-5 catalyst using the PAD method reached almost 100% conversion even at 360 K, which corresponds to the highest catalytic activity and TOF value based on the surface exposed Pt metal.

XAFS measurement was performed to characterize these catalysts. Fig. 3 shows Pt L_{III}-edge XANES and FT-EXAFS spectra. The steeply rising absorption edge is referred to as white line, which reflects the vacancy in the 5d orbital of Pt atoms [16]. A large white line was observed on oxidized Pt, whereas a small white line was observed on reduced Pt (Fig. 3(A), a and b). Therefore, it is possible to estimate the oxidation state of the Pt atom in each sample. The prepared catalysts showed similar white line intensity to the Pt foil in the XANES spectra, indicating that the Pt particle on CeO_2/ZSM-5 was in a metal state. In the FT-EXAFS spectra, the presence of the peak assigned to the Pt–O bond and the Pt–Pt bond were observed at around 1.6 and 2.5 Å, respectively [17]. The prepared catalysts exhibited the only peak due to Pt–Pt bond, suggested the formation of Pt metal. The peak intensity of Pt–Pt bond decreased in the order of Pt foil > imp-Pt/ZSM-5 > PAD-Pt/CeO_2/ZSM-5. This clearly suggests that the smaller Pt metal nanoparticles are formed on the PAD-Pt/CeO_2/ZSM-5 catalyst, which showed higher activity for CO oxidation, compared to the imp-Pt/ZSM-5 catalyst.

In our previous work, the Pt nanoparticles were found to be deposited selectively on the Ti-oxide moieties of Ti-containing mesoporous silica under UV-light irradiation [10]. Fig. 4 shows the TEM image of PAD-Pt/CeO_2/ZSM-5 catalyst. EDX analysis revealed that the Pt nanoparticles selectively deposited on CeO_2 phase in ZSM-5. It is considered that CeO_2 acted as anchor to deposit Pt under UV-light irradiation because CeO_2/ZSM-5 showed absorption in the UV region. The average diameter of the Pt nanoparticles visible in the TEM image is ca. 5 nm, which are slightly larger than 2.0 nm obtained from CO absorption measurement. This observation indicated that the extremely small Pt nanoparticles that cannot be detected by TEM exist within the internal pore of ZSM-5 zeolite.

Moreover, the interaction between Pt nanoparticles and CeO_2 was stronger than that between Pt nanoparticles and ZSM-5 supports, which inhibit the aggregation of Pt nanoparticles [15]. In contrast, Pt nanoparticles on imp-Pt/ZSM-5 showed some aggregates and wide size distribution and the Pt nanoparticle on TiO_2/ZSM-5 are also not so much highly dispersed. The CeO_2 phase plays a crucial role to attain high dispersion of Pt supported catalysts. Until now, Bera et al. have reported that the promoting

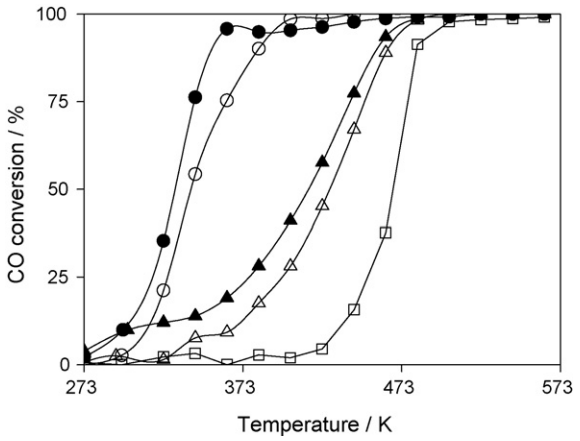

Fig. 2. Catalytic activity for CO oxidation of Pt supported catalysts: (□) imp-Pt/ZSM-5; (△) imp-Pt/TiO_2/ZSM-5; (▲) PAD-Pt/TiO_2/ZSM-5; (○) imp-Pt/CeO_2/ZSM-5; (●) PAD-Pt/CeO_2/ZSM-5 (100 mg catalyst, SV 18000 mL g_{cat}^{-1} h^{-1}).

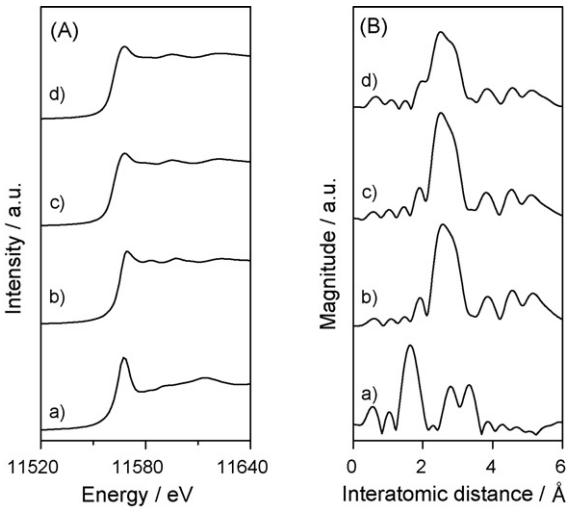

Fig. 3. (A) Pt L_{III}-edge XANES and (B) FT-EXAFS spectra of (a) PtO_2, (b) Pt foil, (c) imp-Pt/ZSM-5, and (d) PAD-Pt/CeO_2/ZSM-5.

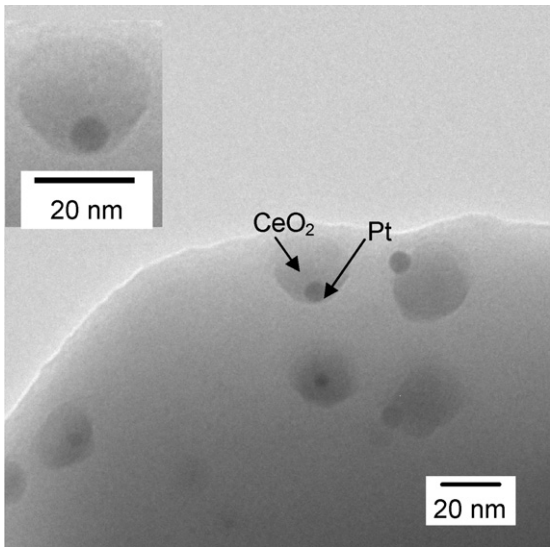

Fig. 4. TEM image of PAD-Pt/CeO_2/ZSM-5 catalyst.

effect of CeO_2 in Pt supported catalysts for CO oxidation, in which the Pt/CeO_2 catalyst acheived 100% conversion at 423 K [18]. In this study, the Pt deposited on CeO_2/ZSM-5 catalyst using the PAD method exhibited high activity even at 360 K. The ZSM-5 has been used as supports of various metal species, Cu, Pd, Pt, and showed high catalytic activities [19–21]. The present system can attain higher catalytic activity for CO oxidation reaction by using CeO_2/ZSM-5 support.

4. Conclusions

In conclusions, nano-sized Pt particles can be successfully deposited on CeO_2/ZSM-5 and TiO_2/ZSM-5 using the PAD method under UV-light irradiation. These catalysts were used for CO oxidation reaction. The highest activity for this catalytic reaction can be attained by Pt/CeO_2/ZSM-5 prepared by the PAD method compared to that prepared by the impregnation method. The results obtained in the present work clearly showed that the promotion effects of CeO_2 and the PAD method are effective for preparation of highly active metal catalysts. The particle size of Pt metal depended on metal oxide phase of catalytic support and significantly affected on catalytic activity for CO oxidation reaction.

Acknowledgements

We are grateful for the financial supports by Priority Assistance for the Formation of Worldwide Renowned Centers of Research – The Global COE Program (Project: Center of Excellence for Advanced Structural and Functional Materials Design) and the Grant-in-Acid for Scientific Research (No. 20360363) from the Ministry of Education, Culture, Sports, Science and Technology (MEXT), Japan. S.S. thanks the JSPS Research Fellowship for Young Scientist. The X-ray adsorption experiments were performed at the High Energy Accelerator Research Organization, KEK, BL-7C station (2007G031, 2007G077). The authors appreciate Dr. Eiji Taguchi and Prof. Hirotaro Mori at the Research Center for Ultra-High Voltage Electron Microscopy, Osaka University for assistance with TEM measurements and Mr. Shigeru Tamiya at the Renovation Center of Instruments for Science Education and Technology, Osaka University for assistance with ICP measurements.

References

[1] J. de Graaf, A.J. van Dillen, K.P. de Jong, D.C. Koningsberger, J. Catal. 203 (2001) 307.
[2] P. Gélin, M. Primet, Appl. Catal. B 39 (2002) 1.
[3] O.S. Alexeev, B.C. Gates, Ind. Eng. Chem. Res. 42 (2003) 1571.
[4] M. Haruta, Chem. Rec. 3 (2003) 75.
[5] E. Bus, J.A. van Bokhoven, Phys. Chem. Chem. Phys. 9 (2007) 2894.
[6] D.K. Liguras, D.I. Kondarides, X.E. Verykios, Appl. Catal. B 43 (2003) 345.
[7] G. Martra, L. Prati, C. Manfredotti, S. Biella, M. Rossi, S. Coluccia, J. Phys. Chem. B 107 (2003) 5453.
[8] P.V. Kamat, Chem. Rev. 93 (1993) 267.
[9] H. Yamashita, K. Mori, Chem. Lett. 36 (2007) 348.
[10] S. Shironita, K. Mori, T. Ohmichi, E. Taguchi, H. Mori, H. Yamashita, J. Nanosci. Nanotechnol. 9 (2009) 557.
[11] H. Yoshida, L. Yuliati, T. Hamajima, T. Hattori, Mater. Trans. 45 (2004) 2062.
[12] T. Blasco, M.A. Camblor, A. Corma, P. Esteve, J.M. Guil, A. Martínez, J.A. Perdigón-Melón, S. Valencia, J. Phys. Chem. B 102 (1998) 75.
[13] M. Wu, G. Lin, D. Chen, G. Wang, D. He, S. Feng, R. Xu, Chem. Mater. 14 (2002) 1974.
[14] J. Zhang, X. Ju, Z.Y. Wu, T. Liu, T.D. Hu, Y.N. Xie, Z.L. Zhang, Chem. Mater. 13 (2001) 4192.
[15] Y. Nagai, T. Hirabayashi, K. Dohmae, N. Takagi, T. Minami, H. Shinjoh, S. Matsumoto, J. Catal. 242 (2006) 103.
[16] H. Yoshida, Y. Yazawa, N. Takagi, A. Satsuma, T. Tanaka, S. Yoshida, T. Hattori, J. Synchrotron Rad. 6 (1999) 471.
[17] S. Imamura, T. Higashihara, Y. Saito, H. Aritani, H. Kanai, Y. Matsumura, N. Tsuda, Catal. Today 50 (1999) 369.
[18] P. Bera, A. Gayen, M.S. Hegde, N.P. Lalla, L. Spadaro, F. Frusteri, F. Arena, J. Phys. Chem. B 107 (2003) 6122.
[19] D.W. Smith, Annu. Rep. Prog. Chem., Sect. A: Inorg. Chem. 100 (2004) 253.
[20] C.-K. Shi, L.-F. Yang, Z.-C. Wang, X.-E. He, J.-X. Cai, G. Li, X.-S. Wang, Appl. Catal. A: Gen. 243 (2003) 379.
[21] M. Kotobuki, A. Watanabe, H. Uchida, H. Yamashita, M. Watanabe, Chem. Lett. 34 (2005) 866.